Development of a Small Molecule Inhibitor of Interleukin-18 for the Prevention of Vein Graft Failure or Other Inflammatory Diseases

Development of a Small Molecular Interleukin-18 Inhibitor for the Prevention of Vein Graft Failure or Other Inflammatory Diseases

Philip LoGerfo

A Thesis in the Field of Biology

for the Degree of Master of Liberal Arts in Extension Studies

Harvard University

March 2019

Abstract

Overexpression of Interleukin-18 (IL18), a pleiotropic pro-inflammatory cytokine has been implicated in the early pathogenesis of intimal hyperplasia (IH), the leading cause of delayed graft failure. IL18 Binding Protein (IL18BP) is the natural inhibitor of IL18. Although recombinant IL-18BP is being clinically tested as a potential therapy to treat IL-18 associated conditions, a small molecule inhibitor of IL-18 may be clinically more amenable and feasible as a potential therapy to prevent IH development or other chronic inflammatory diseases.

Fellow collaborators had previously performed comprehensive *in silico* screening of over 100,000 molecule fragments capable of binding IL18. Sixteen compounds were predicted to stably bind to either IL18 receptor binding sites on the IL18 molecule or other allosteric sites. For this study, *in vitro* IL18 signaling inhibition assays and microscale thermophoresis (MST) protein/ligand binding assays were conducted to discern which of those compounds most effectively bind and inhibit IL18 cell signaling, so that they may be used in further preclinical drug development.

Results from the signaling inhibition assays indicated that 6 of the 16 compounds inhibit IL18 signaling comparably to the positive control IL18BP. Through a series of MST trials, these six also demonstrated significant binding affinity (Kd) with IL18. Interestingly the data suggest that some compounds interact with IL18 not only at different binding sites from one another, but some interact at multiple sites as well. The

results provide evidence for the design of future toxicity and efficacy studies *in vitro* and *in vivo* focused on the most promising inhibitors.

Author's Note

The author of, and fellow collaborators who contributed to, this manuscript have requested an embargo period of two years before its content is made public. No patents for the small molecules, or compounds, mentioned in the manuscript have yet been granted. Additionally, in the manuscript, the scientific names of the compounds are replaced with generic names (i.e. CP1, CP2, CP3, etc.), and no descriptions of the compounds' structures or physical properties are made.

Acknowledgments

The work described in this thesis represents one stage of a project that has evolved over several years, to which many people have contributed. Much gratitude and appreciation are owed to all of them, including the thesis co-directors Leena Pradhan, PhD and Gabriel Birrane, PhD; research advisor James Morris, MD; Finith Jernigan, PhD; Jae Eun Cheong, PhD; Lijun Sun, PhD; Manoj Bhasin, PhD; Akshi Thakkar; Amruta Samant; Özgür Cakici, PhD; Adele Gabba; Kelly Arnett, PhD; Nicole Eckart, PhD of NanoTemper, who assisted with MST analysis for this project; the unknown guy who explained that the MST target temperature can be manually changed; Jesus Revuelta, PhD; Cleide Da Silva, PhD; Herwig Moll, PhD; my boss, Christiane Ferran, MD; and my Dad, Frank LoGerfo, MD.

Table of Contents

Author's Note v

Acknowledgments vi

List of Figures ix

Chapter I. Introduction 1

Vascular Bypass Grafts 1

Background of Procedure 1

Causes of Graft Failure 2

Development and Progression of Intimal Hyperplasia 3

IL18 4

IL18 and Pathogenesis of Vein Graft Failure 4

IL18, Inflammation, and Auto-Immunity 4

Mode of Activation 5

IL18 Receptor Signaling and the IL18BP Regulatory Mechanism 6

Basis for Development of Small Molecular IL18 Inhibitor 7

Hypothesis and Experimental Approach 8

Definition of Terms 10

Chapter II. Materials and Methods 16

Cell Signaling Inhibition Assays 16

Reporter cell line 16

Vehicle preparation and treatment administration 16

Cell assay protocols 17
Microscale Thermophoresis 18
Chapter III. Results 20
Cell Signaling Inhibition Assays 20
Microscale Thermophoresis 21
Limitations 24
Chapter IV. Discussion 27
Conclusion 28
Figures 29
Cell Assay Results 30
MST 34
References 42

List of Figures

Figure 1: Molecular fragment screening cascade. 29

Figure 2: Rendering of IL18 Electrostatic Surface 29

Figure 3A: Most significant results of compounds qualified for further testing. 30

Figure 3B: Cont'd most significant results of compounds qualified for further testing. ...30

Figure 3C: IL18 signaling inhibition results for positive control, IL18BP. 31

Figure 4: Most significant results of compounds disqualified from further testing. 31

Figure 5A: Results from second phase of IL18 signaling inhibition tests. 32

Figure 5B: Cont'd results from second phase of IL18 signaling inhibition tests. 32

Figure 5C: Results for positive control, IL18BP, for second phase of tests. 33

Figure 6: High Binding Affinity Events of Ligands with Multiple Affinities 34

Figure 7: Low Binding Affinity Events of Ligands with Multiple Affinities 35

Figure 8: Ligands compared individually to IL18BP 36

Figure 9: Single High Affinity Binding Event.....40

Chapter I.

Introduction

Vascular Bypass Grafts

Background of Procedure

Vascular bypasses are surgical procedures commonly performed to restore normal blood flow to an area of the body where flow has been reduced due to vascular injury or disease. Bypass procedures are also necessary for organ transplantations and for providing vascular access for hemodialysis patients. In cases of vascular disease, a conduit, or graft, must be implanted that connects healthy vascular regions on each side of a diseased region so that blood flow may be redirected to bypass this region. Coronary artery bypass graft (CABG) and lower extremity vein graft (LEVG) implantations are the two most common types of bypass surgical procedures. The material for the graft is often harvested from a vein of the patient such as the saphenous vein (Conte, M. S., 2007). However, a prosthetic material or a human vein from a donor may be used in some cases.

CABGs are performed to bypass clogged regions of coronary arteries in order to restore blood flow to the heart muscle. LEVGs are intended to restore blood flow to a clogged region in the leg or foot. LEVG surgeries are commonly performed on diabetics and cigarette smokers who are at high risk for peripheral vascular disease, which can cause poor circulation and ulceration in the lower legs and feet. Approximately 250,000 CABG and 80,000 LEVG are performed each year in the United States (Owens, Gasper,

Rahman, & Conte, 2015).

Causes of Graft Failure

While about 50% of CABG and 40% of LEVG fail within 1 year, the causes of delayed graft failure most often originate during the vascular remodeling phase that occurs within the first several weeks following surgery (Ozaki, 2007). The first stage of vascular remodeling is characterized by inflammation that occurs around the vessel walls of the vein graft in response to the trauma of implantation. Inflammation is the immune system's response to a pathology including infections, physical injury, chronic ailments such as diabetes, cardiovascular diseases, cancer etc. In case of physical injuries, inflammation is the initial response that starts the healing process. While inflammation may be caused by any of the reasons listed above, with as many different types of symptoms, similar types of cells and molecules are involved in the inflammatory response. In case of physical injury, including surgery induced injury, successful wound healing requires multiple processes to occur in a timely and coordinated sequence. Extracellular signaling molecules such as cytokines regulate the initiation and resolution of inflammation. However, unresolved or chronic inflammation may occur if signaling patterns are disrupted, thus causing further damage to the original wound.

After vein graft implantation surgery, in addition to the surgical intervention, inflammation is also triggered by the permeation of the graft's endothelial monolayer of cells that lines the lumen of the vessel, and exposure of the endothelium to a new hemodynamic environment (Davies & Hagen, 2011). This happens because the vein in its original anatomy is exposed to low pressures while after the implantation as bypass graft

conduit, it gets exposed to the high arterial pressures. Damaged vascular endothelial cells (ECs) release a surge of cytokines, that signal activation and recruitment of blood platelets and leukocytes such as monocytes and T Cells to the site of injury. Blood platelets will aggregate at the permeated endothelium form a clot, or thrombus to prevent blood loss, and leukocytes assist with thrombus formation by depositing extracellular matrix proteins (ECMs) such as fibrin and collagen to form a connective scaffold (Sur, Sugimoto, & Agrawal, 2014).

Development and Progression of Intimal Hyperplasia

Synthesis and degradation of ECMs in the thrombus is regulated in part by matrix metalloproteinase (MMP) enzymes, which are secreted by the leukocytes. MMPs also stimulate the proliferation and migration of vascular smooth muscle cells (SMCs) from the medial layer of the vessel into the newly forming intimal layer called the neointima. SMCs begin to lose their contractile phenotype as they migrate through the neointima, deposit ECMs, and become more rigid as they are unprotected from the sheer force of blood flow by the endothelium, which has yet to fully repair (Owens et al., 2015).

The continued thickening of the intima and narrowing of the lumen indicates the development of intimal hyperplasia (IH), the leading cause of delayed graft failure (Mitra et al, ‘06, Cox et al, ‘91). While IH will develop in all grafts to some extent, the severity of long-term progression is largely determined by the initial impact of the inflammatory response that begins with cytokine signaling at the site of disrupted endothelium during the first few days following implantation (Wu, Mottola, Schaller, Upchurch, & Conte, 2017).

IL18 and Pathogenesis of Vein Graft Failure

To gain a better understanding of what genes may contribute to the early pathogenesis of vein graft failure, we previously analyzed the transcriptomic changes that occur to ECs and medial SMCs in the first month following vein graft implantation in an *in vivo* canine vein graft model (Bhasin et al., 2012). We observed that Interleukin-18 (IL18) transcriptional expression was significantly upregulated in both SMCs and ECs. In particular for EC it was upregulated for the entire first month following surgery at all five observed time points (2 and 12 hours, 1, 7, and 30 days). Furthermore, IL18 was the only upregulated gene that was involved in at least one enriched disease pathway at all time points, including atherosclerosis signaling, T Cell differentiation, Dendritic cell maturation, and T & B cell signaling, all of which are processes that correspond with IH development (Stoll et al., 1998). Subsequent *in vitro* tests on human saphenous vein EC and SMC also demonstrated a significant increase in cell proliferation and collagen deposition following IL18 treatment, suggesting IL18 contributes to processes that precede IH development.

IL18, Inflammation, and Auto-Immunity

Overexpression of the cytokine IL18 has been implicated in the pathogenesis of many inflammatory and autoimmune diseases, including rheumatoid arthritis, atherosclerosis, lupus, renal disease, and heart disease (Charles A. Dinarello, Novick, Kim, & Kaplanski, 2013; Hutton, Ooi, Holdsworth, & Kitching, 2016; Li et al., 2008). It was first recognized for its ability to induce production of interferon gamma (IFNγ),

another cytokine known to mediate the immune response to viral infections and tumor growth, by natural killer (NK) lymphocytes (Nakamura, Okamura, Wada, Nagata, & Tamura, 1989), which are a component of the innate immune response.

IL18 is now understood to have a range of pleiotropic effects in both innate and adaptive immune responses, and particularly the T helper type 1 (Th1) cell response (Novick et al., 1999). Th1 cells are a class of T helper cells responsible for adaptive immunity. Unlike the innate immune system that responds to pathogens non-specifically, adaptive immunity targets specific pathogens that must become recognized and remembered by the immune system over time. Th1 cells are known to mediate the adaptive immune response to viral and other intracellular pathogens. The Th1 assortment of cytokines differs somewhat from other T helper cell types such as Th2 cells, which mediate antibody production against extracellular pathogens, and Th17 cells that are involved in mucosal immunity. IL18 has also been shown to contribute to Th2 responses to helminthic infections, and also to induce Th1 cells to produce Th2 associated cytokines in a murine asthmatic lung model (Hata, Yoshimoto, Hayashi, Hada, & Nakanishi, 2004; Wiener et al., 2008).

Mode of Activation

IL18 is considered a member of the IL-1 family of cytokines. The protein has a beta-trefoil structure that is similar to IL-1 cytokines, as well as similar activation and receptor signaling mechanisms. Like IL-1β, the IL18 protein has an inactive precursor form that is expressed in the cytosol which must be enzymatically cleaved into its active form by the caspase-1 enzyme before secretion. Caspase-1 is a component of the

inflammasome protein complex (C. A. Dinarello, 2001) that is activated by TLRs and PRRs in response to endotoxins like lipopolysaccharides (LPS). However, unlike IL-1β, which only certain immune cells express, IL-18 is constitutively expressed by most eukaryotic cell types (Keyel, 2014).

IL18 Receptor Signaling and the IL18BP Regulatory Mechanism

IL18 must be engaged by two plasma membrane receptors in a step-wise manner, IL18Rα and then IL18RAP, for signal transduction. Studies suggest that IL18 and IL18Rα must first form a binary complex that IL18RAP can recognize and bind to activate signaling (Tsutsumi et al., 2014). IL18 activity is counter-regulated by an extracellular decoy receptor, IL18 Binding Protein (IL18BP). IL18BP binds with high affinity to IL18, presumably to one of the receptor binding sites, thus neutralizing the biological activity of IL18 by blocking engagement with the receptors (Charles A. Dinarello et al., 2013)

Structural analyses of the IL18 and IL18BP interface indicate that the binding interface is highly conserved across most species. Treatment with recombinant human IL18BP effectively reduced IH progression following balloon-induced arterial injury in an atherosclerotic rabbit model (Li et al., 2008). Poxviruses also take advantage of the conserved binding mechanism by expressing high amounts of IL18BP as a means to evade the host's immune response (Krumm, Meng, Wang, Xiang, & Deng, 2012; Nazarian et al., 2008).

Basis for Development of Small Molecular IL18 Inhibitor

IL18BP has shown therapeutic potential in treating IH and other inflammatory conditions in animal models such as osteoporosis, skin hypersensitivity, and LPS-induced liver injury (Faggioni et al., 2001; Li et al., 2008; Mansoori et al., 2016; Plitz et al., 2003). However, IL18BP treatment has also proven impractical in clinical trials possibly due to poor protein bioavailability as well as protein stability and delivery problems.

Based on this information, development of a stable small molecule that can bind to and inhibit IL18 signaling may help to prevent IH development and other similar inflammatory diseases.

Our group had previously performed *in silico* screening of small molecule fragments (molecular weights between 100-300 Daltons) for potential binding interaction with the IL18 protein. For this screening we obtained publicly available crystal and nuclear magnetic resonance (NMR) structures of IL18 and IL18BP and used software programs designed to predict binding affinity between a given protein structure and known molecular fragments drawn from public databases. After scanning over 100,000 small molecules, we identified sixteen potential inhibitors (Appendix Table 1) predicted to bind either to amino acid residues necessary for IL18/IL18BP interaction, or to residues in allosteric sites on IL18 that may cause a conformational change to the protein structure (Appendix Figure 1).

Recent studies have identified small molecules that may disrupt the binding of IL18 to its receptors by using a similar *in silico* screening technique (Krumm, Meng, Xiang, & Deng, 2017). However, a mechanism of interaction between IL18 and a small molecular antagonist has not been identified. Demonstration that the inhibitory effects are

caused by a specific binding mechanism would be a necessary step to further develop a potential therapeutic use of the antagonist, and begin to assess toxicity and side effects.

Hypothesis and Experimental Approach

The hypothesis for this study states that any compound capable of inhibiting IL18 signaling transduction should do so by directly binding to the IL18 molecule in a manner that disrupts IL18 from interacting with IL18 cell membrane receptors. Thus, two modes of experiments were conducted; one to assess which if any of the 16 compounds may inhibit IL18 signaling, and another set to measure strength of interaction and binding between IL18 and whichever molecules demonstrate signaling inhibition. The signaling inhibition assays consisted of a bio-assay that employed a HEK293-derived cell line (HEK-Blue IL18, Invivogen,, USA) with genes encoding IL18 receptors (IL18R and IL18RAP) and a SEAP (secreted embryonic alkaline phosphatase) reporter gene, which is expressed in specific response to IL18 signaling. Cells were treated with IL18 and potential inhibitors or the positive control, IL18BP, and SEAP production was measured thereafter, as described in Materials and Methods.

With the 6 remaining compounds that demonstrated signaling inhibition, protein-ligand interaction assays were performed using microscale thermophoresis (MST). Microscale Thermopheresis (MST) is an immobilization-free technology that measures biomolecular interactions with a wide range of affinities (pM-mM). The MST instrument detects the motion of fluorescently labelled molecules, over a certain time period, along a microscopic temperature gradient induced by an infrared laser aimed at the centers of

specially designed capillaries. Typically, 16 capillaries are prepared for one experiment, with each consecutive capillary containing a two-fold diluted concentration of an un-labelled ligand along with a fixed concentration of fluorescently labelled target molecule. By detecting shifts in fluorescence levels between the capillaries, the instrument can measure changes in the molecular hydration shell, charge, or size that may be caused by ligand interaction with the target molecule. From this information the instrument calculates a dissociation constant (Kd), expressed in molar units, to describe the ligand-protein binding affinity. Thus, the binding affinities between each of the 6 potential ligands and fluorescently labelled IL18 were measured and compared to that of the positive control, IL18BP.

Definition of Terms

Adaptive Immunity: Immune responses that develop specifically to attack certain pathogens that avoid detection or resolution by the innate immune response. Adaptive immunity employs T and B cells known as memory cells, which develop to recognize specific antigens, so that the immune system can respond more efficiently to a pathogen following the system's initial encounter with it.

Atherosclerosis: A vascular disease characterized by narrowing of the lumen and hardening of the vessel walls caused by accumulation of plaques. The debris of dead cells and connective tissue that results from intimal hyperplasia (IH) development also contributes to atherosclerotic plaque buildup.

Coronary Artery Bypass Graft (CABG): A surgically implanted graft that bypasses blocked coronary arteries in order to restore normal blood flow to the heart. Graft material may consist of a healthy vein or artery transplanted from another part of the body, or a prosthetic (synthetic) material.

Caspase-1: Enzyme that cleaves the inactive precursors of IL-18 and IL-1β into their active forms. It is a component of the inflammasome protein complex.

Collagen: A protein found in extracellular matrix (ECM) throughout the body that provides structural support. Collagen is also important for providing a platform for cell migration in wound healing.

Cytokine: A broad family of intercellular signaling proteins that are secreted from cells

and interact with specific receptors on cell surfaces. Cytokines play a primary role in regulating immune responses. Most nucleated cells can produce some types of cytokines.

Dissociation Constant (Kd): Expressed in molar units, it is the concentration of a ligand at which the concentration of protein with ligand bound equals the concentration of unbound protein.

Vascular Endothelial Cells (EC): Simple squamous cells that comprise the thin monolayer of cells known as the endothelium of the vessel. The endothelium acts as a barrier between the blood circulating through the lumen of the blood vessel and the vessel wall. Lymphatic vessels also have an endothelium.

Extra Cellular Matrix (ECM): Network of molecules that comprise the supporting and connective tissues with in and around organs, by regulating stiffness and elasticity.

Fibrin: A fibrous protein that bind to platelets and help with clot formation.

Interferon gamma (IFNγ): A cytokine that activates immune cells to respond to infectious pathogens. IL-18 signaling is known to induce certain immune cells to express IFNγ.

Interleukin-18 Receptor Accessory Protein (IL18RAP): One of the two receptor subunits that comprise the IL18 receptor complex. IL18RAP and IL18Rα form a heterodimer that engages IL18 at the cell membrane surface to form a ternary complex that enables IL18 signal transduction.

Interleukin-18 Receptor Alpha (IL18Rα): One of the two receptor subunits that comprise the IL18 receptor complex. IL18 presumably encounters IL18Rα prior to being engaged by a second receptor subunit IL18RAP that enables signal transduction.

Interleukin-1 beta (IL1β): A proinflammatory cytokine that is similar to IL18 in its structure, function, and mode of activation. Both cytokines are expressed in response to some but not all of the same pathogens. IL-1 β is produced primarily by immune cells, whereas IL-18 is produced by most types of cells.

Innate Immunity: The immune system's initial response, which involves a range of lymphocytes that will identify and attack infections and other foreign substances. Unlike with adaptive immunity, the response is nonspecific to any particular pathogen, and as no memory of previous pathogens is retained by the innate immune system.

Interleukin-18 (IL18): A cytokine that induces an inflammatory immune response to fight infections and resolve injury. Unregulated overexpression of IL18 has been associated with many inflammatory and autoimmune disorders.

Intima: The innermost layer of a blood vessel wall. It consists of the vascular endothelium that is in contact with the blood flow, and a supportive elastic membrane (internal elastic lamina), consisting mostly of SMCs, that is in contact with the outer medial layer of the vessel.

Leukocytes: The broad family of immune cells that provide a protective response to foreign pathogens. Leukocytes are produced in the bone marrow and circulate throughout the vascular and lymph systems. Also known as white blood cells.

Lower Extremity Vein Graft (LEVG): A surgically implanted graft that bypasses blocked coronary arteries in the leg in order to restore circulation and salvage lower limbs in patients with peripheral artery disease. Graft material may consist of a healthy vein or artery transplanted from another part of the body, or a prosthetic material.

Lipopolysaccharide (LPS): Large molecules containing a lipid and a polysaccharide. They are expressed on the surface of many types of bacteria. Detection of LPS by TLRs can induce production of IL18.

Lumen: The inner space of a vessel through which blood flows.

Matrix Metalloproteinases (MMP): Enzymes that can process, cleave and/or degrade a wide range of proteins, including ECMs, cytokines, and receptors that are involved in tissue remodeling and wound healing.

Microscale Thermophoresis (MST): an immobilization-free technology that detects the motion and physical changes of fluorescently labelled molecules caused by interactions with a ligand along a microscopic temperature gradient over a certain time period.

NF-κB: Family of transcription factors that bind to DNA in the cell nucleus to promote gene transcription. NF-κB transcription factors primarily regulate the expression of genes associated with inflammatory and innate immune responses.

Natural Killer Cells (NK): A type of lymphocyte that is part of the innate immune response against viral-infected cells and other harmful types of stimuli. NK cells can be induced by IL-18 to express IFNγ.

Neointima: A newly formed intimal layer of the blood vessel wall towards the lumen of the blood vessel that develops following vascular injury and damage to the endothelium.

Pattern Recognition Receptors (PRR): A large family of cell membrane receptors that are part of the innate immune system. PRRs detect many types of foreign pathogens as well as debris from damaged cells and tissue.

Platelets: Non-nucleated cell fragments that circulate in the blood and prevent bleeding following injury by forming clots. They are produced in the bone marrow by megakaryocytes.

Saphenous Vein: The longest vein in the body that runs along the medial side of the leg, from the big toe to the femur. Portions of the saphenous vein are commonly used as grafts for vascular bypass surgeries because they are generally autologous and fail at a lesser rate than prosthetic materials.

T Cells: A subfamily of leukocytes that play dynamic roles in mediating the immune response. T Cells may direct the actions of other immune cells by secreting certain cytokines in response to specific pathogens. Some T Cells may also directly attack pathogens.

Th1 Cells: A subgroup of T Cells known to mediate the adaptive immune response to viral and other intracellular pathogens

Th17 Cells: A subgroup of T Cells that mediate immunity to pathogens found in the mucus.

Th2 Cells: A subgroup of T Cells that mediate antibody production against extracellular pathogens

Toll Like Receptors (TLR): A subgroup of PRRs that are expressed on cell membranes. TLRs contribute to the innate immune response by detecting the presence of microbes.

Vascular Smooth Muscle Cells (SMC): Myocytes found within the blood vessel walls that regulate blood flow through contraction and relaxation. Following vascular injury,

SMCs lose their contractile phenotype, migrate into the luminal area of the blood vessels, proliferate, become synthetic, and secrete extracellular matrix proteins (ECM) as part of the remodeling process. Unregulated migration, proliferation and ECM deposition by SMC can lead to the development of intimal hyperplasia.

Chapter II.

Materials and Methods

Cell Signaling Inhibition Assays

Reporter cell line

HEK-Blue IL18 Cells (Invivogen California, USA), are a derivative of HEK293 cells that have been stably transfected with IL18Rα/IL18RAP genes and a SEAP reporter gene that is expressed and secreted in specific response to IL18. Cells were grown in 25mm^2 tissue culture flasks with DMEM culture medium containing 4.5 g/l glucose, 10 % (v/v) heat-inactivated fetal bovine serum, 50 U/ml penicillin, 50 µg/ml streptomycin, 100 µg/ml Normocin and 2 mM L-glutamine at 37 °C in 5 % CO2.

Vehicle preparation and treatment administration

Stock concentration of IL18 was 750µM stored in Tris-HCL buffer at -80°C. Aliquots for cell treatments were diluted in sterile H^2O to 1.6 µM and stored at -80°C. For treatment use, aliquots were further diluted in H^2O to 100 times the intended treatment concentration and administered into wells containing 198µl media at volumes of 2µl to yield the correct treatment concentration. Compounds were solubilized and stored in DMSO at stock concentrations between 2.5-250mM. For treatment use, compounds were diluted in sterile PBS to 100 times the intended treatment concentration and administered into wells containing 198µl media at volumes of 2µl. Total DMSO contents for all vehicles was less than .02% prior to treatment, and less than .0002% within wells

following treatment.

Cell assay protocols

HEK-Blue IL18 cells were transferred from flasks and seeded at 40-50% confluency on 96-well culture plates 6 hours prior to treatment. For the initial pilot test phase, wells were treated with a selected compound at concentrations of 3.75nM, 7.5pM, and 1.5pM, with three replicate wells for each concentration, and six replicate wells with no compound treatment (NT). All wells were then immediately co-treated with recombinant human IL18 at one concentration between 15pM-100pM. Following treatments, cells were incubated at 37 °C in 5 % CO2 for 18 hours. Cell confluency typically reached 70-80% (~80,000-100,000 cells per well) by this point, 24 hours after seeding.

For the second phase of reporter assays the six most potent inhibitory compounds were tested at least once with the following protocol: six replicate wells treated with a selected compound at a low dose range (800pM, 200pM, 50pM, 12.5pM, NT, plus 50pM IL18 co-treatment) and a higher dose range (1600pM, 400pM, 100pM, 25pM, NT, plus 100pM IL18 treatment).

To detect SEAP activity, 20 µl supernatant from each well was transferred and mixed with 180 µl alkaline phosphatase detection medium (QUANTi-Blue, InvivoGen, California, USA), in a separate 96-well plate and incubated for 3 hours at room temperature. Supernatant SEAP activity was measured by reading the optical density (OD) at 640nm using a spectrophotometer. OD values were standardized to NT mean = 1.

Statistical analysis was performed GraphPad Prism (California, USA) software. One-Way analysis of variance (ANOVA) with Dunnett's post-hoc analysis was used to

determine significant variation between treatment and control (NT) groups treated only with IL18.

Microscale Thermophoresis

Recombinant IL18 was fluorescently labelled using the lysine reactive Pico RED NT647 dye from NanoTemper Technologies and stored in a PBS buffer containing 0.05% TWEEN (Buffer A). Stock concentration of labelled IL18 was 10μM. Working concentrations of IL18 were diluted in Buffer A to 10, 40, or 50nM. Except for the positive control, IL18BP, stock concentration for all compounds, or ligands, was 10-25mM in 100% DMSO. Ligands were diluted in Buffer A to working concentrations of 50-500 μM. containing 0.8-2% DMSO. Stock concentration of IL18BP, was 50μM, stored in 20mM Tris-HCl buffer (pH 8.0) containing 0.4 M Urea and 10% glycerol (Buffer B). Prior to MST experiments being performed 16 preparations of two-fold serial dilutions of ligand in uniform buffer, starting with the working ligand concentration, were incubated with equal volumes of a fixed concentration of labelled IL18. After 30 minutes incubation at room temperature, 16 Monolith NT.115 standard capillaries were loaded with 10μl volumes of each of the ligand/IL18 preparations. Tests described in Results were run at 37°C.

Experiments were performed on a Monolith NT.115Pico machine (NanoTemper Technologies GmbH, Germany). Data quality and analysis and graphic rendering were performed using MO.Affinity Analysis v2.3 software from NanoTemper technologies. Evaluation strategy for all analyses was standardized to measure relative change of

fluorescence (FNorm %) over the first 2.5 seconds of laser induced temperature shift per capillary. Statistical analysis was performed using the software's provided Kd analysis method.

Chapter III.

Results

Cell Signaling Inhibition Assays

The initial round of in vitro IL18 signaling inhibition assays were intended to determine which of the 16 compounds demonstrated sufficient potential to be examined further in both the MST binding assays and additional signaling inhibition assays. Due to time and resource constraints, each compound could only be tested two times in initial in vitro assays, and a maximum of 6 compounds would be considered for further analysis if so many showed enough promise. For these tests, Hek-Blue cells were treated with a compound at relatively high concentrations (37.5, 7.5nM, and 1.5nM). As cell SEAP reporter expression was highly sensitive to IL18 signaling, cells were then immediately co-treated with IL18 at either a low (15-40pM) or slightly higher concentration (50-100pM).

Surprisingly, 8 of the 16 compounds demonstrated statistically significant signaling inhibition for at least one dosage treatment compare to untreated (NT) controls in any assay. All six compounds chosen for further analysis inhibited signaling at multiple concentrations (Figures 3A, 3B), comparable to the positive control, IL18BP (Figure 3C). Nevertheless, several unchosen compounds showed effects trending toward

significance and may have deserved further analysis had time and resources permitted (Figure 4).

The second phase of *in vitro* assays tested the remaining 6 compounds at lower treatment concentrations to verify consistent inhibitory effects, and also attempt to determine a minimum concentration threshold for effectiveness. While the compounds continued to inhibit significantly at all concentrations (800, 200, 50, 25pM) when co-treated with 50pM IL18, a dose dependent curve of effectiveness could not be determined for any of them (Figures 5A, 5B). A dose dependent curve was also not observed for IL18BP (Figure 5C). This inability to find dose dependent curves may signify one of the technical limitations of the assay as discussed in the next Chapter.

Microscale Thermophoresis

Figures 6 thru 8 depict the relative change in fluorescence detection (FNorm), measured as percentage, caused by a laser induced temperature gradient over period of 2.5 seconds within the capillaries at different ligand concentrations. As the lysine residues on the surface of IL18 have been fluorescently labelled, this change in fluorescence suggests physical alterations to IL18 have occurred during the time period. MST trials with 4 of the 6 compounds (CP3, CP5, CP11, CP16) exhibited two concentration dependent shifts in IL18 fluorescence, which appear as biphasic curves separated by plateaus, as seen in Figures 6 and 7. Figure 6 highlights the early downward curves that occur at low ligand concentrations, and Figure 7 shows the later downward curves at higher concentrations. For MST experiments, the early biphasic curve usually

suggests a high affinity ligand binding event. The later curve is caused by a lower affinity binding event that can only occur at high ligand concentrations. The plateau between the curves indicates that interaction at the high affinity binding site has reached its saturation point, while the ligand concentration is still too low for the ligands to interact with the protein at the lower affinity site. While multiple interactions may be advantageous in some contexts, in drug development such binding promiscuity may be a forewarning of unintended drug effects.

Figure 8 shows the FNorm curves for each compound in comparison with that of the positive control IL18BP. In figure 8A, CP3 demonstrates a biphasic curve with a strong reduction on fluorescence detection, even more so than IL18BP. However, the mean level of reduction may be caused a variety of undetermined factors as discussed in Limitations. The binding affinity (Kd) for CP3 was estimated at 60.6nM with a Kd confidence ± 68.2nM, as shown in Figure 8G. The estimated Kd for IL18BP was 1.85nM with a strong confidence ±1.04nM.

Results for CP4 (Figure 8B) show a significant downward FNorm reduction at low concentrations, suggesting a high affinity binding event. However, higher concentrations show sporadic FNorm values which may suggest poor solubility, or ligand dimerization that prevents interaction with IL18 these higher concentrations. While Kd is calculated at 2.27nM for CP4, the relatively wide confidence value (±4.16nM) reflects the sporadic measurements at higher concentrations.

CP5 (Figure 8C) possibly displays a biphasic curve, but further repetitions of trials may be needed to verify this occurrence. Nonetheless, at higher concentrations, a low affinity event is clearly observed that follows distinctly different trajectory from that

of the positive control. This may indicate a binding event occurring at a site other than the IL18BP/IL18 binding site, as this particular compound was previously predicted to bind at an allosteric site of the protein (data not shown). While the binding affinity is calculated to be the weakest of the tested compounds (5.64μM), the relatively slim confidence value (2.71μM) suggests consistent binding event.

Results from the trials with CP9 shown in Figure 8D depict a single high affinity binding event. The FNorm trajectory also most clearly resembles that of the positive control. While the Kd score was lowest of all compounds (0.56nM) including IL18BP, however the wide Kd confidence value (1.33nM) indicates the need for more test repetitions. Figure 9 shows CP9 again with an overlay of an additional test using lower IL18 (5nM) and ligand (25μM) concentrations and higher LED excitation power (20%) than the previous tests to more accurately determine the binding affinity (6.09nM). The FNorm trajectory was in line those from the previous tests.

CP11 and CP16 (Figure 8E, 8F) both clearly demonstrate biphasic curves, with early and later binding events. For CP11 overall Kd was 14.9nM, with early and later events calculated at 0.76nM and 1.25μM, respectively, as shown in Dataset Overviews of Figures 6 and 7. Overall Kd for CP16 was 13.1nM, with early and later events calculated at 0.53nM and 7.65 μM, respectively.

Limitations

According to the manufacturer specifications, HEK Blue IL18 cells express SEAP in response to IL18 treatments ranging from 10pg/ml to 1ng/ml, or 0.5 to 50pM, approximately. Considering this, it may have been more informative to test the neutralizing effects of compounds by using lower treatment concentrations of both IL18 and the compounds. For the second phase of tests, cells were treated with 50pM (data shown) and 100pM (data not shown). At 100pM, neither IL18BP nor the compounds demonstrated any consistent inhibitory effect. However, the relatively high treatment concentrations still cannot explain why no dose dependent curves were observed for any of the compounds nor IL18BP when co-treated 50pM IL18. For all of them 12.5pM treatment was approximately as effective as 50, 200, and 800pM.

Unfortunately, no publications show results from any experiments utilizing HEK-Blue cells designed specifically for IL18 induced SEAP activity. HEK-Blue cells have been used extensively to measure SEAP induced TLR signaling in other studies of anti-inflammatory compounds (Cai et al., 2018; Xu et al., 2018), but treatment doses used in the published experiments are mostly in micromolar ranges. Experiments with IL1β specific HEK-Blue cells have been published as well (Dietsch et al., 2016; Yang et al., 2014), but these cells reach saturation of SEAP activity at 100ng/ml doses of human IL1β (www.invivogen.com/hek-blue-il1b), about 100 times higher than the saturation point for HEK-Blue IL-18 cells.

MST technology holds many advantages over other ligand binding assay technologies. For one, assays require far smaller volumes and concentrations of molecules and buffer materials than most binding assays, which makes it an efficient method to determine the presence of ligand interaction. The MST machine also allows for temperature settings to be adjusted, which can have a significant effect on the molecular binding and behavior. The results shown for this study all came from tests run at 37C to match normal body temperature. However, several rounds of preliminary tests were performed at the default default temperature of 22°C, yielding far less consistent results at considerably higher Kd values for the test compounds, mostly between ~1-100μM (data not shown). Even the positive control did yield lower Kd values compared the test compounds at 22°C, IL18BP still Kd was still roughly higher (~30-100nM) than at 37°C.

As with other assays that use fluorescent labelling of amino acid residues, the potential for interference with ligand interaction by the labelling material must be considered. Furthermore, for MST, several variables can affect quality of fluorescent labelling depending on the structure and amino acid composition of the protein, such as unlabelled stock concentrations, final labelled concentrations, and timing of the desalting process. all vary considerably. Early MST experiments were also discarded from analysis due to poor protein labelling, which required the MST machine to use excessively high excitation power to detect fluorescence, thus resulting in high levels of photobleaching and a low signal to noise ratio.

MST results, while comprehensive and informative, require high degree of knowledge of the machine's calculation methods in order to interpret the data. As mentioned in the results, for instance, the mean level of FNorm reduction may be

misinterpreted to mean that a ligand has a more interactive effect on the protein structure, a seen with CP3 compared to IL18BP. However, the lower mean FNorm may reflect more sensitive fluorescence detection due to a higher concentration of fluorescently labelled protein, or a combination of other factors, such as MST measurement time and power, and signal to noise ratio. In Figures 6 and 7 for instance, another pair of tests with CP3 are depicted, which were run with a lower fixed IL18 concentration of 5nM, instead of 20nM, and show a higher mean FNorm.

Chapter IV.

Discussion

Utilizing small molecules as protein-protein inhibitors has emerged as a new method of drug discovery and development (Wilson & Arkin, 2011). To disrupt protein-protein interaction, specific locations on a protein through which a protein interfaces with other molecules must be identified. IL18 is known to interact with three proteins; IL18Ra and IL18RAP comprise the cell membrane bound receptor subunits which are required for signal transduction; IL18BP inhibits, or neutralizes IL18 bioactivity, by competitively binding IL18 at the same regions at which the receptors would bind. Previous studies have identified three distinct regions on IL18 through which the protein interacts with the receptors and IL18BP (Meng, Leman, & Xiang, 2007). Two are required for IL18Ra binding and a third region required for IL18RAP binding. It has been shown that variola virus derived IL18BP interacts at all three regions (Kato et al., 2003).

Within the protein-protein binding regions, proteins interact with high affinity at certain locations of key amino acid residues. Small molecules can advantageously disrupt this interaction by competitively binding at these key residue sites. However, the entire binding regions on which the proteins interface span a vast area, measuring on average 1,600 ± 400 Angstroms(Å)^2 of surface area, and they are predominantly hydrophobic in nature. In fact, the IL18/IL18BP has been shown to span ~1,930 Å^2 of surface area (Krumm et al., 2017). Such large-scale hydrophobic interaction poses a challenge for small molecule drug development. To overcome this, drug developers of cytokine inhibitors have attempted to combine additional low affinity molecules targeting different

residue sites with one high affinity, or lead molecule, targeting a primary site (Braisted et al., 2003; He et al., 2005; Wilson & Arkin, 2011).

Conclusion

Here, we have identified 6 out of 16 candidate molecules that significantly inhibit IL18 signaling *in vitro*. In future functional analysis studies, discarded human saphenous veins will be tested *ex vivo* for inhibition of IFNγ expression following co-treatments with the compounds and IL18. A series of MST experiments also demonstrated that one of these six compounds, CP9, appears to bind IL18 at a single high affinity site, with Kd comparable to that of IL18BP, while others interact at multiple sites, suggesting occurrences of promiscuous binding to different regions of the protein. Nonetheless, additional MST testing must be performed with all six compounds to more accurately discern the ligand-protein Kd at high and/or low affinities. Additionally, crystallization of these ligand protein complexes would clarify the locations of these interactions, and whether or not combinations of ligands on a larger molecular platform would be practical in future drug development.

Figures

Figure 1: Molecular fragment screening cascade.

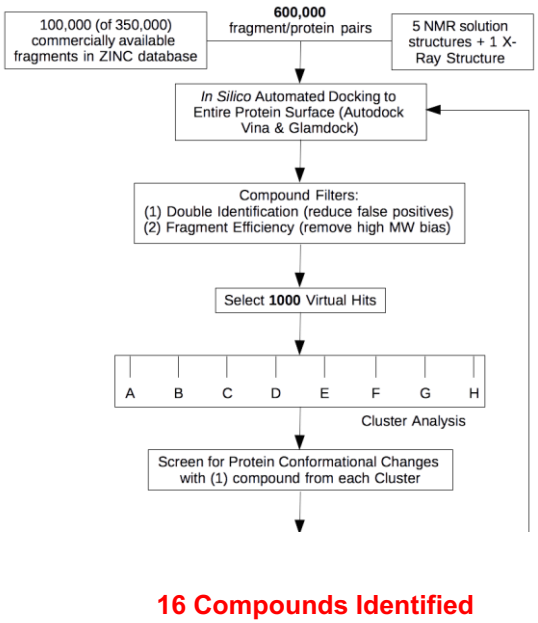

Screening cascade for the identification of fragments capable of binding IL18. Courtesy, Finith Jernigan

Figure 2: Rendering of IL18 Electrostatic Surface

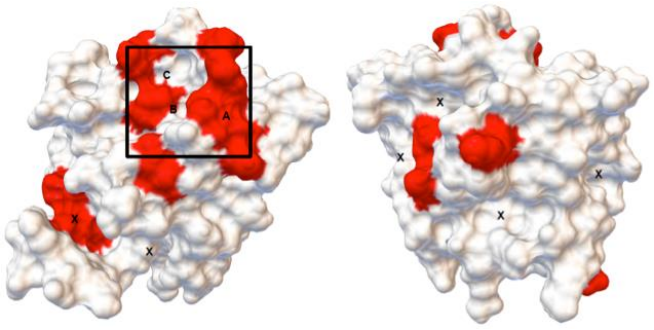

Figure 2: Front (Left) and Rear (Right) space filling view of IL-18. Amino acid residues important for IL-18BP binding are highlighted in RED. Black box indicates binding site of IL-18. Potential allosteric binding sites are labeled with (X). Courtesy, Finith Jernigan.

Figure 3A: Most significant results of compounds qualified for further testing.

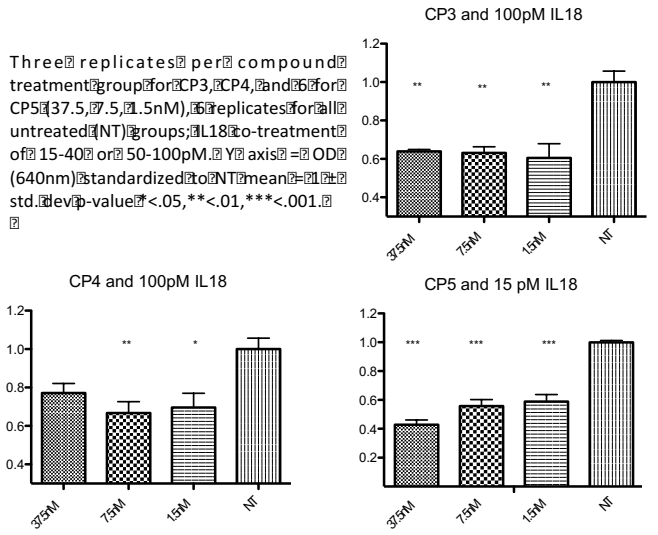

Figure 3B: Cont'd most significant results of compounds qualified for further testing.

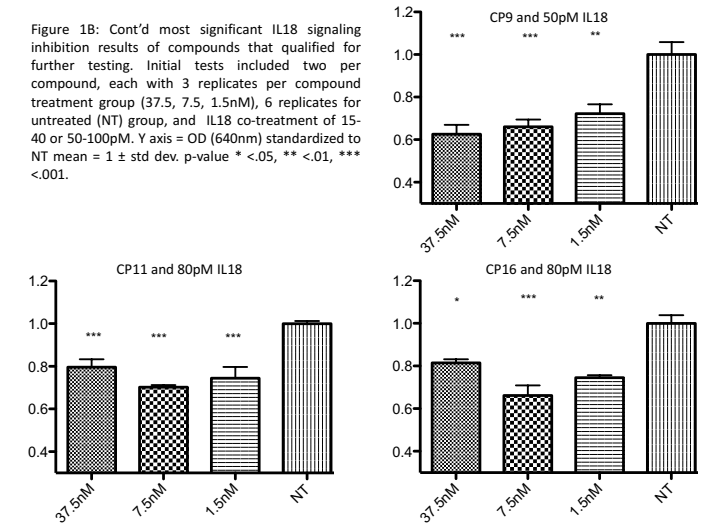

Figure 3C: IL18 signaling inhibition results for positive control, IL18BP.

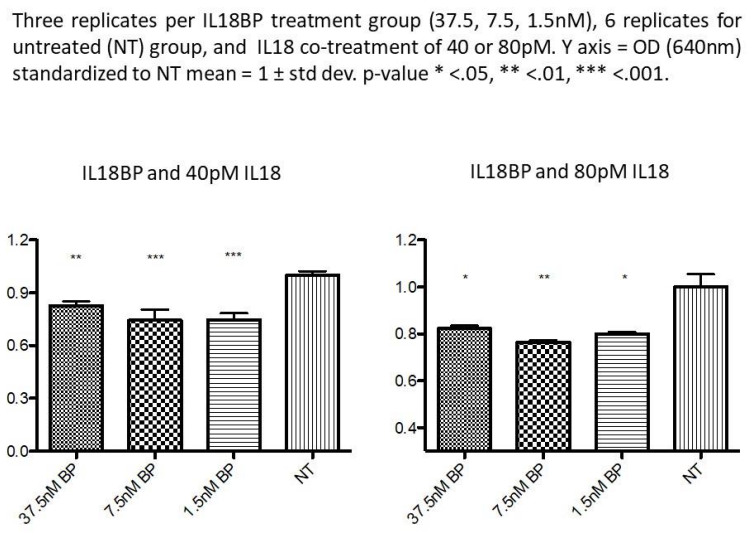

Figure 4: Most significant results of compounds disqualified from further testing.

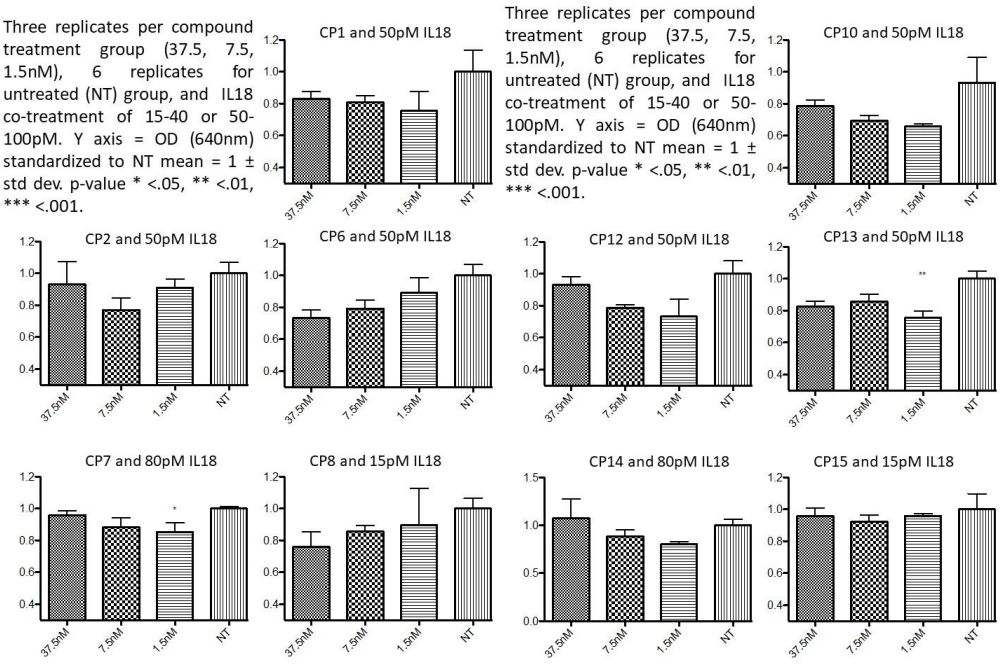

Figure 5A: Results from second phase of IL18 signaling inhibition tests.

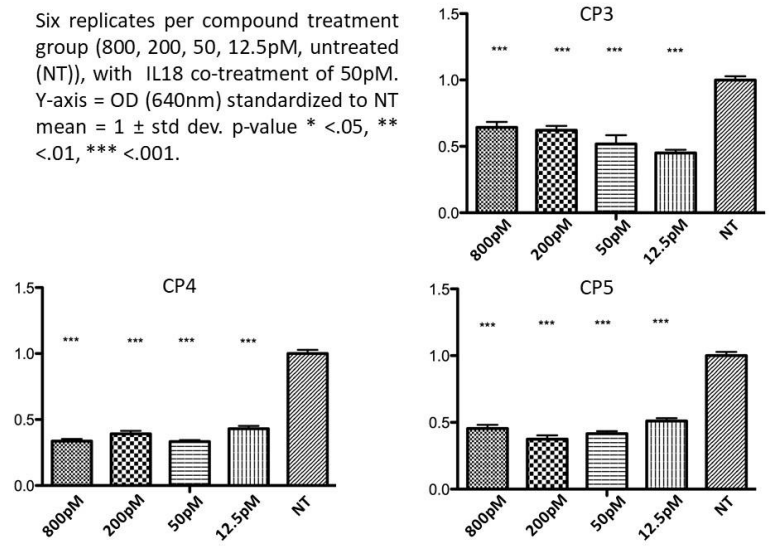

Figure 5B: Cont'd results from second phase of IL18 signaling inhibition tests.

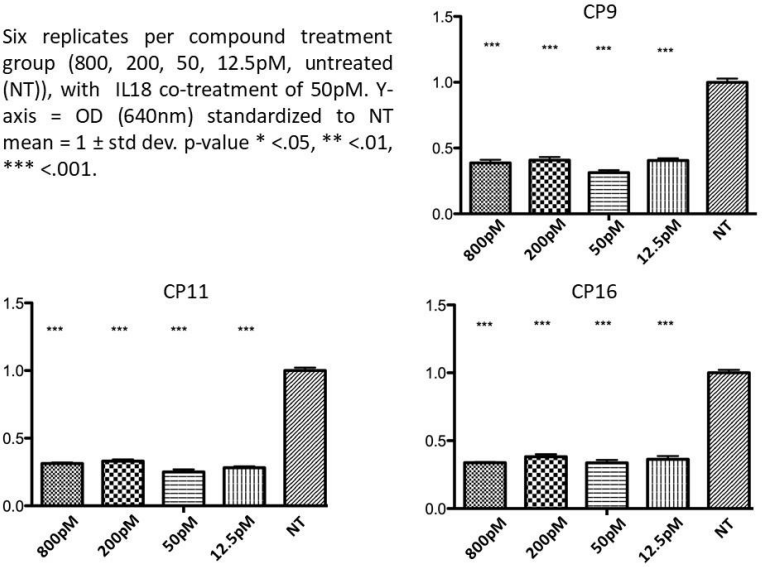

Figure 5C: Results for positive control, IL18BP, for second phase of tests.

Six replicates per IL18BP treatment group (800, 200, 50, 12.5pM, untreated (NT)), with IL18 co-treatment of 50pM. Y-axis = OD (640nm) standardized to NT mean = 1 ± std dev. p-value * <.05, ** <.01, *** <.001.

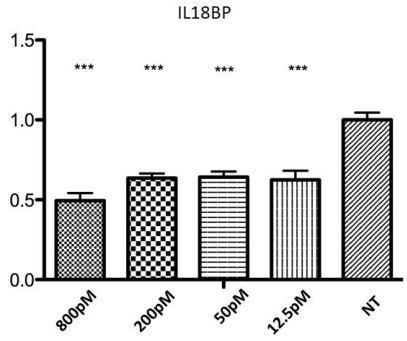

Figure 6: High Binding Affinity Events of Ligands with Multiple Affinities

A) Depicts first phase of biphasic curves, occurring at low ligand concentrations. Higher ligand concentrations are removed from analysis and colored grey.

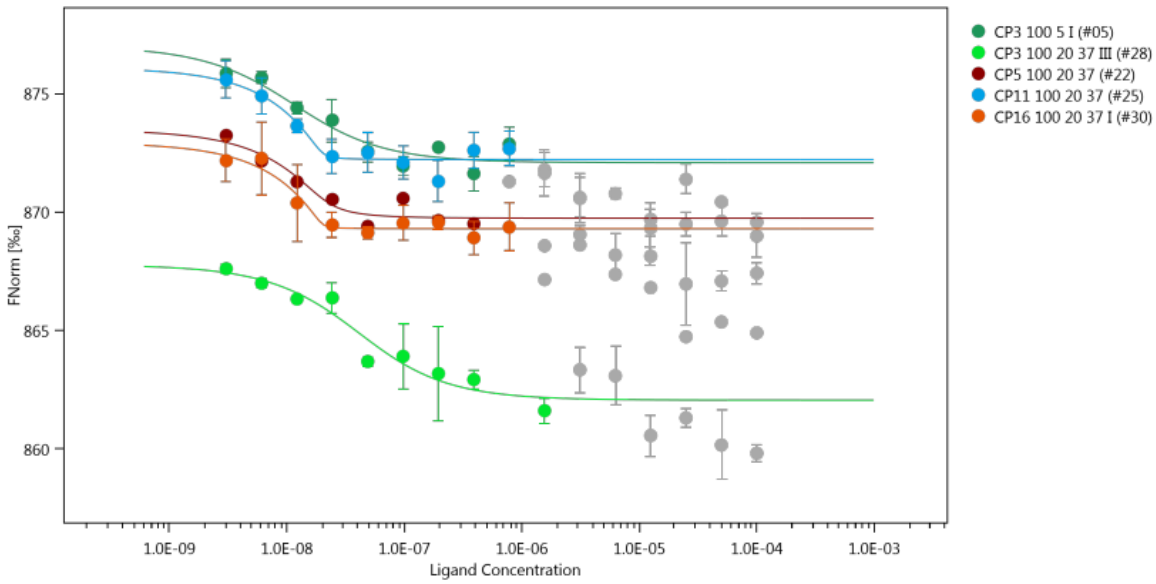

B) Data Set Overview

Name:	CP3 100 5 I (#05)	CP3 100 20 37 III (#28)	CP5 100 20 37 (#22)	CP11 100 20 37 (#25)	CP16 100 20 37 I (#30)
Graph Color:	•	•	•	•	•
Target Name:	IL18	IL18	IL18	IL18	IL18
Target Concentration:	5nM	20nM	20nM	20nM	20nM
Ligand Name:	CP3	CP3	CP5	CP11	CP16
Ligand Concentration:	0.781µM to 0.00305µM	1.56µM to 0.00305µM	1.56µM to 0.00305µM	0.781µM to 0.00305µM	0.781µM to 0.00305µM
n:	2	2	2	2	2
Comments:					
Excitation Power:	20%	5%	5%	5%	5%
MST Power:	40%	40%	40%	40%	40%
Temperature:	37.0°C	37.0°C	37.0°C	37.0°C	37.0°C
Kd:	8.9528E-09	3.0634E-08	1.7067E-10	1.2279E-10	6.8768E-11
Kd Confidence:	± 5.7946E-09	± 1.5676E-08	± 1.2347E-09	± 7.6087E-10	± 5.2775E-10
Response Amplitude:	4.9134166	5.7017699	3.7266994	3.8661909	3.6228481
TargetConc:	5E-09[Fixed]	2E-08[Fixed]	2E-08[Fixed]	2E-08[Fixed]	2E-08[Fixed]
Unbound:	876.99	867.77	874.87	876.08	872.92
Bound:	872.08	862.06	871.14	872.21	869.29
Std. Error of Regression:	0.53811546	0.58823072	0.70425418	0.47020026	0.33551565
Reduced χ^2:	14.017204	177.52979	4.8544944	0.34789274	0.33515378
Signal to Noise:	10.543322	11.19261	6.0002198	9.4944496	12.468285

Figure 7: Low Binding Affinity Events of Ligands with Multiple Affinities

A) Depicts second phase of biphasic curves, occurring at high ligand concentrations. Lower ligand concentrations are removed from analysis and colored grey.

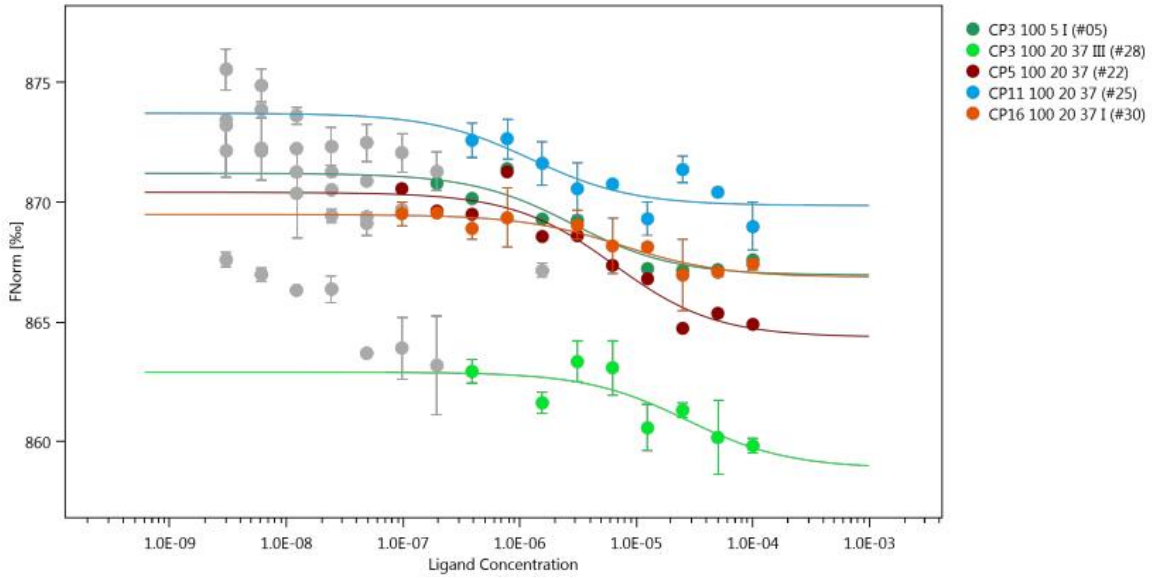

B) Data Set Overview

Name:	CP3 100 5 I (#05)	CP3 100 20 37 III (#28)	CP5 100 20 37 (#22)	CP11 100 20 37 (#25)	CP16 100 20 37 I (#30)
Graph Color:					
Target Name:	IL18	IL18	IL18	IL18	IL18
Target Concentration:	5nM	20nM	20nM	20nM	20nM
Ligand Name:	CP3	CP3	CP5	CP11	CP16
Ligand Concentration:	100µM to 0.195µM	100µM to 0.391µM	100µM to 3.13µM	100µM to 0.391µM	100µM to 0.0977µM
n:	1	2	2	2	2
Comments:					
Excitation Power:	20%	5%	5%	5%	5%
MST Power:	40%	40%	40%	40%	40%
Temperature:	37.0°C	37.0°C	37.0°C	37.0°C	37.0°C
Kd:	2.8643E-06	2.7374E-05	7.4755E-06	1.2542E-06	7.6546E-06
Kd Confidence:	± 2.0001E-06	± 4.0296E-05	± 3.5271E-06	± 1.7757E-06	± 4.2612E-06
Response Amplitude:	4.2528751	4.0222485	7.4228306	3.8594759	2.6168077
TargetConc:	5E-09[Fixed]	2E-08[Fixed]	2E-08[Fixed]	2E-08[Fixed]	2E-08[Fixed]
Unbound:	871.22	862.91	872.29	873.73	869.49
Bound:	866.96	858.88	864.87	869.87	866.87
Std. Error of Regression:	0.62723797	0.89657194	0.33554301	0.82570786	0.34853921
Reduced χ^2:		2.1590158	4.7285954	8.9845687	2.7520595
Signal to Noise:	7.8292409	5.3082061	28.559179	5.3972344	8.5131916

Figure 8: Ligands compared individually to IL18BP

A) CP3 and IL18BP.

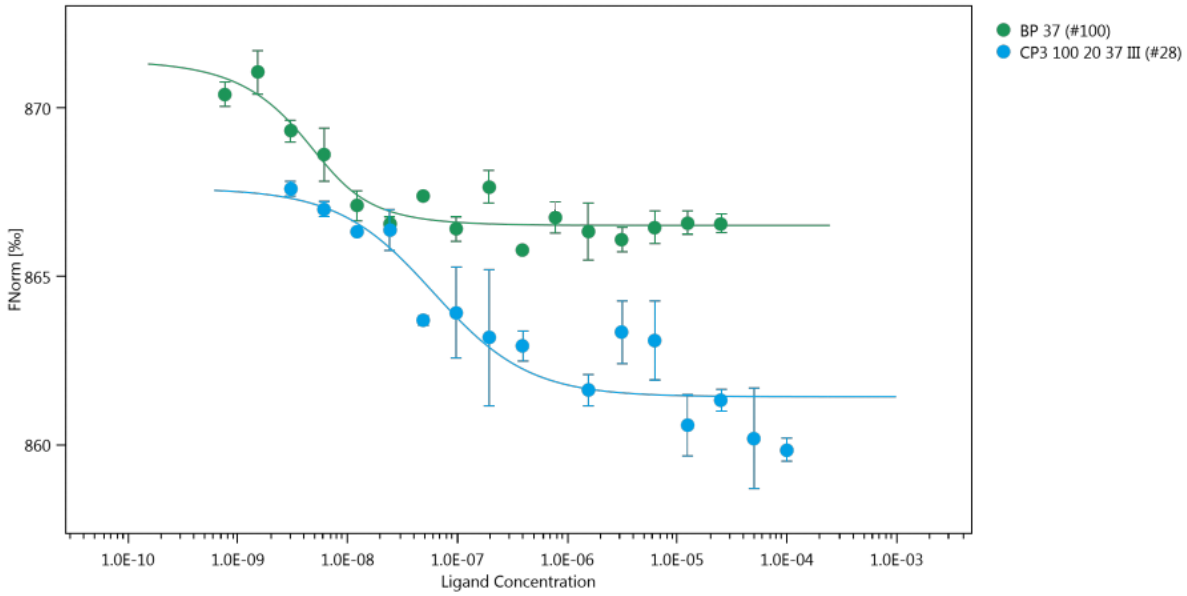

B) CP4 and IL18BP

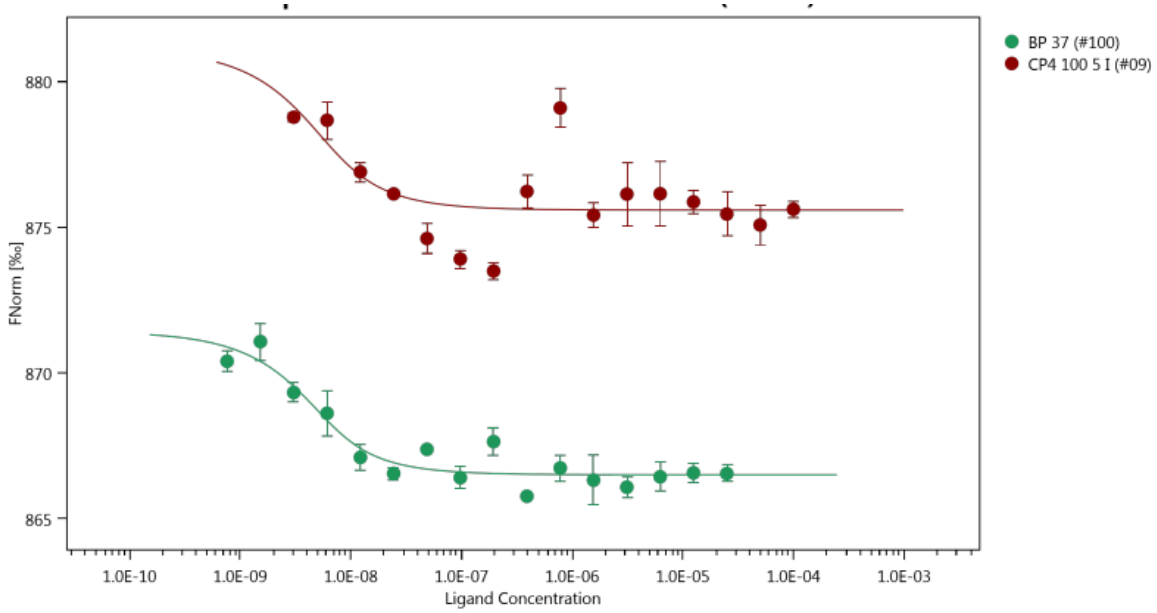

C) CP5 and IL18BP

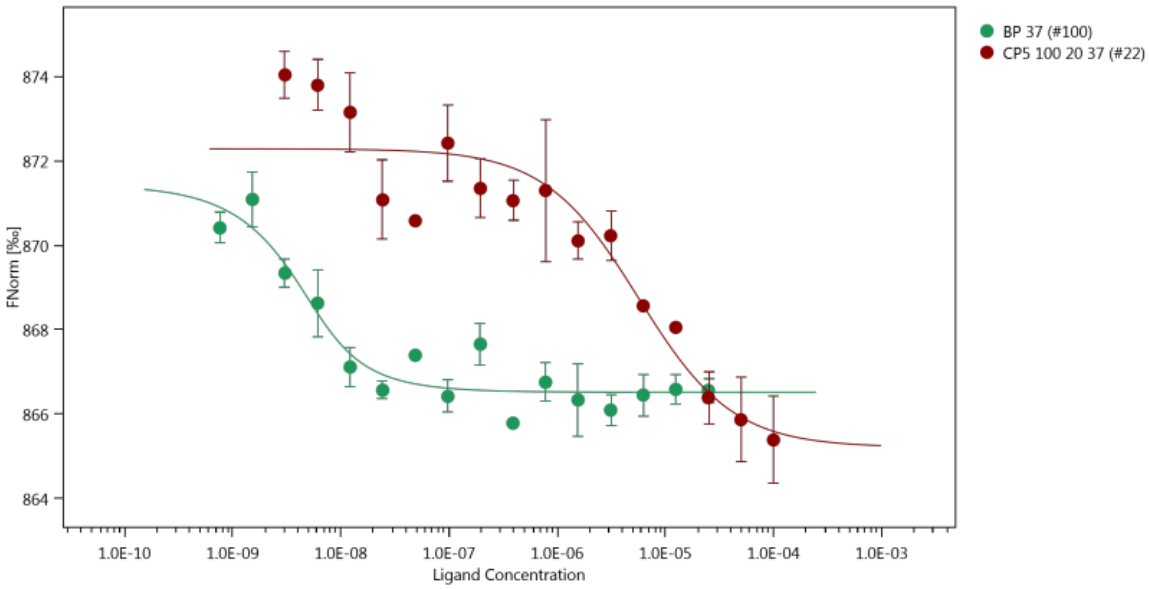

D) CP9 and IL18BP

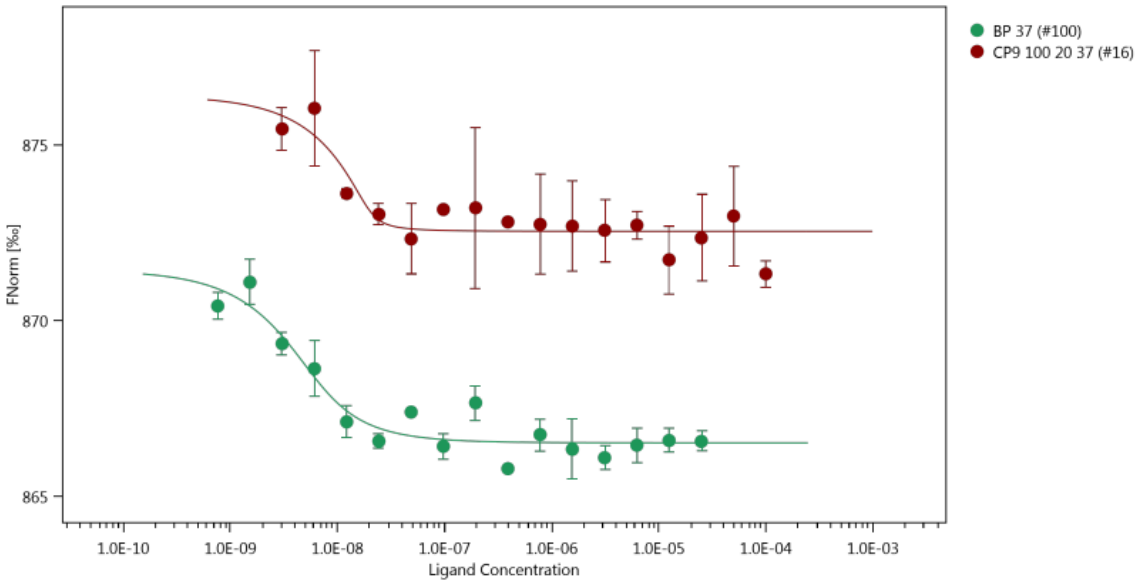

E) CP11 and IL18BP

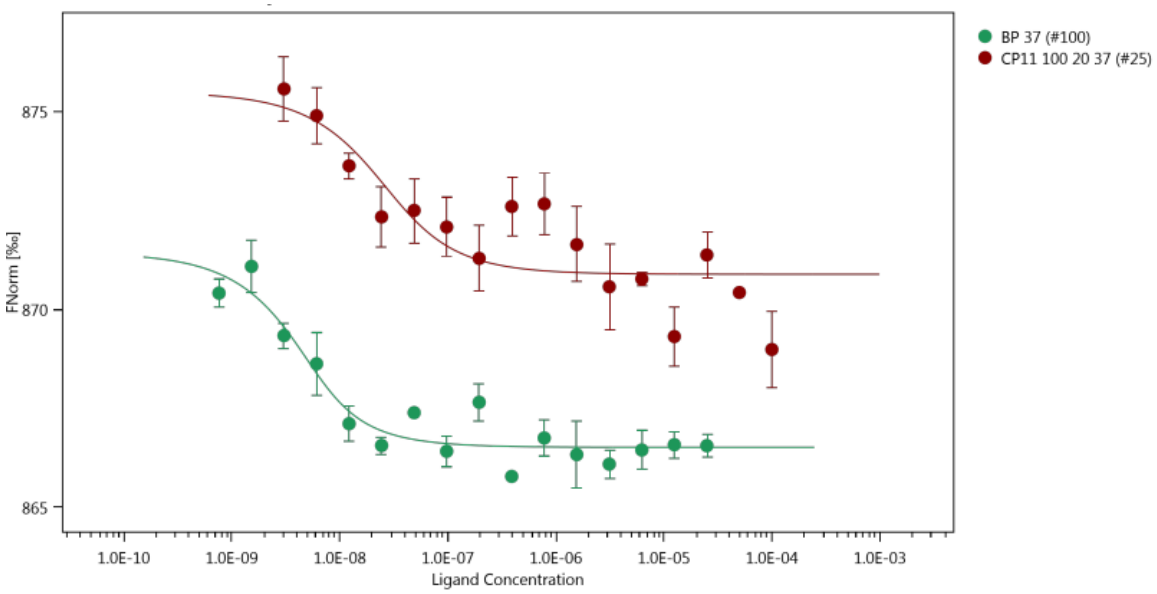

F) CP16 and IL18BP

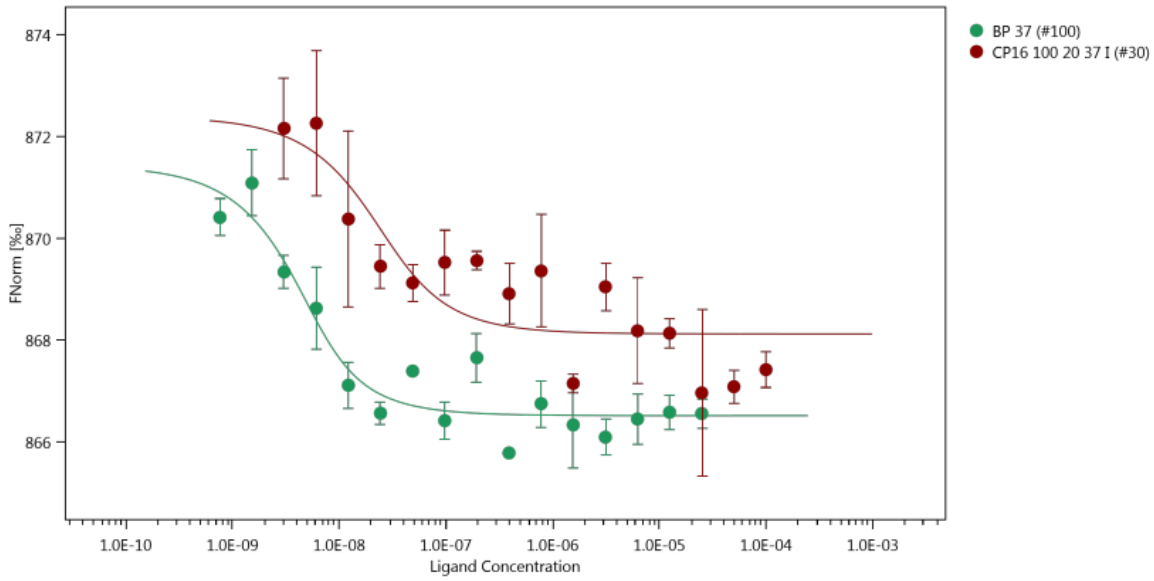

G) Data Set Overview

Name:	IL18BP	CP3	CP4	CP5
Graph Color:	●	●	●	●
Target Name:	IL18	IL18	IL18	IL18
Target Concentration:	5nM	20nM	5nM	20nM
Ligand Name:	BP	CP3	CP4	CP5
Ligand Concentration:	25µM to 0.000763µM	100µM to 0.00305µM	100µM to 0.00305µM	100µM to 0.00305µM
n:	2	2	2	2
Comments:				
Excitation Power:	20%	5%	20%	5%
MST Power:	40%	40%	40%	40%
Temperature:	37.0°C	37.0°C	37.0°C	37.0°C
Kd:	1.8469E-09	6.0575E-08	2.2711E-09	5.6441E-06
Kd Confidence:	± 1.0427E-09	± 6.8251E-08	± 4.1613E-09	± 2.7051E-06
Response Amplitude:	4.9133364	6.2004726	5.5261596	7.0733491
TargetConc:	5E-09[Fixed]	1.3693E-15	5E-09[Fixed]	2E-08[Fixed]
Unbound:	871.43	867.62	881.12	872.28
Bound:	866.52	861.42	875.59	865.21
Std. Error of Regression:	0.52447759	1.0917105	1.3511843	0.98154729
Reduced χ^2:	20.871973	13.716328	10.456252	144.08809
Signal to Noise:	10.062908	6.4074464	4.3932183	7.7408351

Name:	CP9	CP11	CP16	CP9
Graph Color:	●	●	●	●
Target Name:	IL18	IL18	IL18	IL18
Target Concentration:	10nM	20nM	20nM	5nM
Ligand Name:	CP9	CP11	CP16	CP9
Ligand Concentration:	100µM to 0.00305µM	100µM to 0.00305µM	100µM to 0.00305µM	25µM to 0.000763µM
n:	2	2	2	1
Comments:				
Excitation Power:	5%	5%	5%	20%
MST Power:	40%	40%	40%	40%
Temperature:	37.0°C	37.0°C	37.0°C	37.0°C
Kd:	5.4581E-10	1.4962E-08	1.3059E-08	6.0909E-09
Kd Confidence:	± 1.3313E-09	± 1.4986E-08	± 1.2242E-08	± 4.5127E-09
Response Amplitude:	3.859	4.5961831	4.2683509	5.0217917
TargetConc:	2E-08[Fixed]	2E-08[Fixed]	2E-08[Fixed]	5E-09[Fixed]
Unbound:	876.39	875.48	872.39	877.39
Bound:	872.53	870.88	868.12	872.37
Std. Error of Regression:	0.58577295	1.0346993	0.87256359	0.92201717
Reduced χ^2:		14.095453	7.8420713	
Signal to Noise:	7.0765147	4.7715239	5.2545676	5.8505088

Figure 9: Single High Affinity Binding Event

A) CP9 at 5% (n=2) and 20% (n= 1) Excitation Power

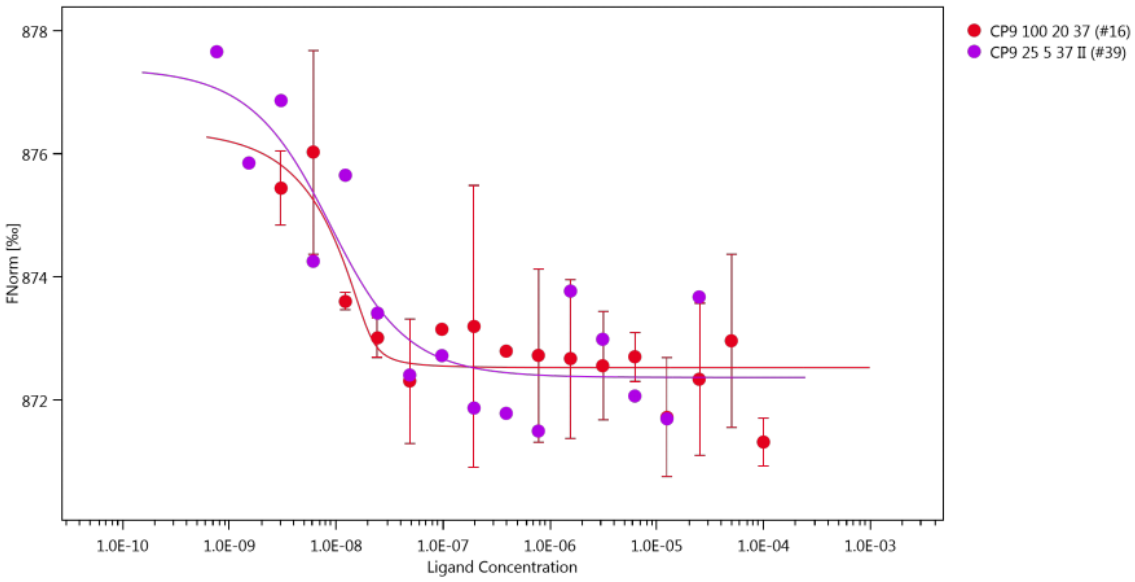

B) Data Set Overview

Name:	CP9 100 20 37 (#16)	CP9 25 5 37 II (#39)
Graph Color:	•	•
Target Name:	IL18	IL18
Target Concentration:	10nM	5nM
Ligand Name:	CP9	CP9
Ligand Concentration:	100µM to 0.00305µM	25µM to 0.000763µM
n:	2	1
Comments:		
Excitation Power:	5%	20%
MST Power:	40%	40%
Temperature:	37.0°C	37.0°C
Kd:	5.4581E-10	6.0909E-09
Kd Confidence:	± 1.3313E-09	± 4.5127E-09
Response Amplitude:	3.859	5.0217917
TargetConc:	2E-08[Fixed]	5E-09[Fixed]
Unbound:	876.39	877.39
Bound:	872.53	872.37
Std. Error of Regression:	0.58577295	0.92201717
Reduced χ^2:		
Signal to Noise:	7.0765147	5.8505088

References

Bhasin, M., Huang, Z., Pradhan-Nabzdyk, L., Malek, J. Y., LoGerfo, P. J., Contreras, M., … LoGerfo, F. W. (2012). Temporal network based analysis of cell specific vein graft transcriptome defines key pathways and hub genes in implantation injury. *PloS One*, *7*(6), e39123. https://doi.org/10.1371/journal.pone.0039123

Braisted, A. C., Oslob, J. D., Delano, W. L., Hyde, J., McDowell, R. S., Waal, N., … Raimundo, B. C. (2003). Discovery of a potent small molecule IL-2 inhibitor through fragment assembly. *Journal of the American Chemical Society*, *125*(13), 3714–3715. https://doi.org/10.1021/ja034247i

Cai, S., Zhu, G., Cen, X., Bi, J., Zhang, J., Tang, X., … Cheng, K. (2018). Synthesis, structure-activity relationships and preliminary mechanism study of N-benzylideneaniline derivatives as potential TLR2 inhibitors. *Bioorganic & Medicinal Chemistry*, *26*(8), 2041–2050. https://doi.org/10.1016/j.bmc.2018.03.001

Davies, M. G., & Hagen, P.-O. (2011). Reprinted article "Pathophysiology of vein graft failure: a review." *European Journal of Vascular and Endovascular Surgery: The Official Journal of the European Society for Vascular Surgery*, *42 Suppl 1*, S19-29. https://doi.org/10.1016/j.ejvs.2011.06.013

Dietsch, G. N., Lu, H., Yang, Y., Morishima, C., Chow, L. Q., Disis, M. L., & Hershberg, R. M. (2016). Coordinated Activation of Toll-Like Receptor8 (TLR8) and NLRP3 by the TLR8

Agonist, VTX-2337, Ignites Tumoricidal Natural Killer Cell Activity. *PloS One*, *11*(2), e0148764. https://doi.org/10.1371/journal.pone.0148764

Dinarello, C. A. (2001). Novel targets for interleukin 18 binding protein. *Annals of the Rheumatic Diseases*, *60 Suppl 3*, iii18-24.

Dinarello, Charles A., Novick, D., Kim, S., & Kaplanski, G. (2013). Interleukin-18 and IL-18 binding protein. *Frontiers in Immunology*, *4*, 289. https://doi.org/10.3389/fimmu.2013.00289

Faggioni, R., Cattley, R. C., Guo, J., Flores, S., Brown, H., Qi, M., … Senaldi, G. (2001). IL-18-binding protein protects against lipopolysaccharide- induced lethality and prevents the development of Fas/Fas ligand-mediated models of liver disease in mice. *Journal of Immunology (Baltimore, Md.: 1950)*, *167*(10), 5913–5920.

Hata, H., Yoshimoto, T., Hayashi, N., Hada, T., & Nakanishi, K. (2004). IL-18 together with anti-CD3 antibody induces human Th1 cells to produce Th1- and Th2-cytokines and IL-8. *International Immunology*, *16*(12), 1733–1739. https://doi.org/10.1093/intimm/dxh174

He, M. M., Smith, A. S., Oslob, J. D., Flanagan, W. M., Braisted, A. C., Whitty, A., … Cunningham, B. C. (2005). Small-molecule inhibition of TNF-alpha. *Science (New York, N.Y.)*, *310*(5750), 1022–1025. https://doi.org/10.1126/science.1116304

Hutton, H. L., Ooi, J. D., Holdsworth, S. R., & Kitching, A. R. (2016). The NLRP3 inflammasome in kidney disease and autoimmunity. *Nephrology (Carlton, Vic.)*, *21*(9), 736–744. https://doi.org/10.1111/nep.12785

Kato, Z., Jee, J., Shikano, H., Mishima, M., Ohki, I., Ohnishi, H., … Shirakawa, M. (2003). The structure and binding mode of interleukin-18. *Nature Structural Biology*, *10*(11), 966–971. https://doi.org/10.1038/nsb993

Keyel, P. A. (2014). How is inflammation initiated? Individual influences of IL-1, IL-18 and HMGB1. *Cytokine*, *69*(1), 136–145. https://doi.org/10.1016/j.cyto.2014.03.007

Krumm, B., Meng, X., Wang, Z., Xiang, Y., & Deng, J. (2012). A unique bivalent binding and inhibition mechanism by the yatapoxvirus interleukin 18 binding protein. *PLoS Pathogens*, *8*(8), e1002876. https://doi.org/10.1371/journal.ppat.1002876

Krumm, B., Meng, X., Xiang, Y., & Deng, J. (2017). Identification of small molecule inhibitors of Interleukin-18. *Scientific Reports*, *7*(1), 483. https://doi.org/10.1038/s41598-017-00532-x

Li, J.-M., Eslami, M. H., Rohrer, M. J., Dargon, P., Joris, I., Hendricks, G., … Cutler, B. S. (2008). Interleukin 18 binding protein (IL18-BP) inhibits neointimal hyperplasia after balloon injury in an atherosclerotic rabbit model. *Journal of Vascular Surgery*, *47*(5), 1048–1057. https://doi.org/10.1016/j.jvs.2007.12.005

Mansoori, M. N., Shukla, P., Kakaji, M., Tyagi, A. M., Srivastava, K., Shukla, M., … Singh, D. (2016). IL-18BP is decreased in osteoporotic women: Prevents Inflammasome mediated IL-18 activation and reduces Th17 differentiation. *Scientific Reports*, *6*, 33680. https://doi.org/10.1038/srep33680

Meng, X., Leman, M., & Xiang, Y. (2007). Variola virus IL-18 binding protein interacts with three human IL-18 residues that are part of a binding site for human IL-18 receptor alpha subunit. *Virology*, *358*(1), 211–220. https://doi.org/10.1016/j.virol.2006.08.019

Nakamura, K., Okamura, H., Wada, M., Nagata, K., & Tamura, T. (1989). Endotoxin-induced serum factor that stimulates gamma interferon production. *Infection and Immunity*, *57*(2), 590–595.

Nazarian, S. H., Rahman, M. M., Werden, S. J., Villeneuve, D., Meng, X., Brunetti, C., … McFadden, G. (2008). Yaba monkey tumor virus encodes a functional inhibitor of interleukin-18. *Journal of Virology*, *82*(1), 522–528. https://doi.org/10.1128/JVI.00688-07

Novick, D., Kim, S. H., Fantuzzi, G., Reznikov, L. L., Dinarello, C. A., & Rubinstein, M. (1999). Interleukin-18 binding protein: a novel modulator of the Th1 cytokine response. *Immunity*, *10*(1), 127–136.

Owens, C. D., Gasper, W. J., Rahman, A. S., & Conte, M. S. (2015). Vein graft failure. *Journal of Vascular Surgery*, *61*(1), 203–216. https://doi.org/10.1016/j.jvs.2013.08.019

Ozaki, C. K. (2007). Cytokines and the early vein graft: strategies to enhance durability. *Journal of Vascular Surgery*, *45 Suppl A*, A92-98. https://doi.org/10.1016/j.jvs.2007.02.032

Plitz, T., Saint-Mézard, P., Satho, M., Herren, S., Waltzinger, C., de Carvalho Bittencourt, M., … Chvatchko, Y. (2003). IL-18 binding protein protects against contact hypersensitivity. *Journal of Immunology (Baltimore, Md.: 1950)*, *171*(3), 1164–1171.

Stoll, S., Jonuleit, H., Schmitt, E., Müller, G., Yamauchi, H., Kurimoto, M., … Enk, A. H. (1998). Production of functional IL-18 by different subtypes of murine and human dendritic cells (DC): DC-derived IL-18 enhances IL-12-dependent Th1 development. *European Journal of Immunology*, *28*(10), 3231–3239. https://doi.org/10.1002/(SICI)1521-4141(199810)28:10<3231::AID-IMMU3231>3.0.CO;2-Q

Sur, S., Sugimoto, J. T., & Agrawal, D. K. (2014). Coronary artery bypass graft: why is the saphenous vein prone to intimal hyperplasia? *Canadian Journal of Physiology and Pharmacology*, *92*(7), 531–545. https://doi.org/10.1139/cjpp-2013-0445

Tsutsumi, N., Kimura, T., Arita, K., Ariyoshi, M., Ohnishi, H., Yamamoto, T., … Kato, Z. (2014). The structural basis for receptor recognition of human interleukin-18. *Nature Communications*, *5*, 5340. https://doi.org/10.1038/ncomms6340

Wiener, Z., Pocza, P., Racz, M., Nagy, G., Tolgyesi, G., Molnar, V., … Falus, A. (2008). IL-18 induces a marked gene expression profile change and increased Ccl1 (I-309) production in mouse mucosal mast cell homologs. *International Immunology*, *20*(12), 1565–1573. https://doi.org/10.1093/intimm/dxn115

Wilson, C. G. M., & Arkin, M. R. (2011). Small-molecule inhibitors of IL-2/IL-2R: lessons learned and applied. *Current Topics in Microbiology and Immunology*, *348*, 25–59. https://doi.org/10.1007/82_2010_93

Wu, B., Mottola, G., Schaller, M., Upchurch, G. R., & Conte, M. S. (2017). Resolution of vascular injury: Specialized lipid mediators and their evolving therapeutic implications. *Molecular Aspects of Medicine*, *58*, 72–82. https://doi.org/10.1016/j.mam.2017.07.005

Xu, Y., Chen, S., Cao, Y., Zhou, P., Chen, Z., & Cheng, K. (2018). Discovery of novel small molecule TLR4 inhibitors as potent anti-inflammatory agents. *European Journal of Medicinal Chemistry*, *154*, 253–266. https://doi.org/10.1016/j.ejmech.2018.05.033

Yang, Y., Inatsuka, C., Gad, E., Disis, M. L., Standish, L. J., Pugh, N., … Lu, H. (2014). Protein-bound polysaccharide-K induces IL-1β via TLR2 and NLRP3 inflammasome activation. *Innate Immunity*, *20*(8), 857–866. https://doi.org/10.1177/1753425913513814